American Mineralogist, Volume 90, pages 1375–1383, 2005

Synthesis and crystal-chemistry of alkali amphiboles in the system Na_2O-MgO-FeO-Fe_2O_3-SiO_2-H_2O as a function of f_{O_2}

GIANCARLO DELLA VENTURA,[1,*] GIANLUCA IEZZI,[2,†] GÜNTHER J. REDHAMMER,[3] FRANK C. HAWTHORNE,[4] BRUNO SCAILLET,[5] AND DANIELA NOVEMBRE[6]

[1]Dipartimento di Scienze Geologiche, Università di Roma Tre, Largo S. Leonardo Murialdo 1, I-00146, Italy
[2]Bayerisches GeoInstitut, Bayreuth, Germany
[3]Institute of Crystallography, Rheinisch-Westfälische-Technische Hochschule Aachen, Jägerstrasse 17-19, D-52056 Aachen, Germany
[4]Department of Geological Sciences, University of Manitoba, Winnipeg, Manitoba, R3T 2N2 Canada
[5]ISTO, UMR 6113, 1A, Rue de la Férollerie, F-45071 Orléans Cedex 2, France
[6]Dipartimento di Scienze della Terra, Università "G. D'Annunzio," I-66013 Chieti Scalo, Italy

ABSTRACT

This paper reports the results of hydrothermal synthesis in the system Na_2O-MgO-FeO-Fe_2O_3-SiO_2-H_2O. Four samples of stoichiometric magnesioriebeckite composition, ideally $\square Na_2Mg_3Fe^{3+}_2Si_8O_{22}(OH)_2$, were run at 700–800 °C, 0.4 GPa, and redox conditions varying from NNO (Nickel–Nickel Oxide) to NNO + 2.3 log f_{O_2}. Powder XRD and SEM-EDX show a high (>85%) amphibole yield for all samples; however, in no case was the end-member composition attained. EMP analyses show that the amphiboles obtained deviate strongly from nominal stoichiometry toward magnesio-arfvedsonite [$NaNa_2Mg_4Fe^{3+}Si_8O_{22}(OH)_2$]. Powder XRD patterns were indexed in the space group *C*2/*m*; refined cell-parameters reflect variations in the amphibole composition, and the cell volume is correlated linearly with the A-site occupancy. Mössbauer spectra show that in all samples, Fe^{3+} is completely ordered at M2, whereas Fe^{2+} occurs at the M1, M3, and M4 sites. The Fe^{3+}/Fe^{2+} ratio is a function of f_{O_2}: for increasing oxidation conditions, there is significant increase in $^{M2}Fe^{3+}$ and decrease in Fe^{2+}, notably in $^{M4}Fe^{2+}$. Mössbauer spectra also show significant variation in $^{M1}Fe^{2+}$ and $^{M3}Fe^{2+}$ quadrupole splitting as a function of the Fe^{3+} content in the amphibole. IR spectra in the OH-stretching region show a well-resolved quadruplet at frequencies <3680 cm^{-1}, assigned to octahedral ^{M1,3}(Mg, Fe^{2+})-OH-$^{A}\square$ configurations, and a broad band consisting of four overlapping components related to ^{M1,3}(Mg, Fe^{2+}) configurations associated with occupied A-sites. Quantitative evaluation of the relative band intensities suggests a linear increase of A-site occupancy with decreasing f_{O_2} of synthesis. The composition of the amphiboles synthesized, can be best described by a combination of the $^{C}(Mg,Fe^{2+})_1$ $^{B}(Mg,Fe^{2+})_1$ $^{C}Fe^{3+}_{-1}$ $^{B}Na_{-1}$ and the $^{A}Na_1$ $^{C}(Mg,Fe^{2+})_1$ $^{A}\square_{-1}$ $^{C}Fe^{3+}_{-1}$ exchange vectors. The experimental trend is in accord with the trend documented for natural amphiboles, and suggests that the amphibole composition can in fact be used to monitor changes in f_{O_2} during crystallization.

INTRODUCTION

Riebeckite is an Na-Fe amphibole found in a wide variety of geological environments. Magnesioriebeckite is characteristic of schists, alkali granites, and syenites (Borley 1963; Lyons 1976; Kovalenko 1968), and asbestiform varieties of magnesioriebeckite have been reported from metasomatized calcareous dolomites and Fe-rich sediments (e.g., see Deer et al. 1997 for a detailed list of occurrences). The standard formula for amphiboles is written as $A_{0-1}B_2C_5T_8O_{22}(O,OH,F)_2$, where A refers to the alkali-cation at the alkali-site (which may show variable occupancy), B refers to cations at the six- to eightfold coordinated M4 site(s), C refers to the M(1,2,3) octahedral cations, and T refers to the tetrahedral cations (Leake et al. 1997).

The ideal formula of magnesioriebeckite is $\square Na_2Mg_3Fe^{3+}_2Si_8O_{22}(OH)_2$, and there is complete solid-solution between this end-member composition and riebeckite [$\square Na_2Fe^{3+}_3Fe^{3+}_2Si_8O_{22}(OH)_2$] (Deer et al. 1997). Complete solid-solution also occurs between riebeckite and arfvedsonite, $NaNa_2(Mg,Fe^{2+})_4Fe^{3+}Si_8O_{22}(OH)_2$ (Kovalenko 1968). Lyons (1976) studied the crystal-chemistry of a series of alkali amphiboles (riebeckites to arfvedsonites) from the granite batholiths of Rhode Island and Massachusetts, and found that the higher temperature of crystallization favor the filling of the A-site in these minerals. Henley (1978) described the occurrence of titanian-arfvedsonite in some basalt dikes from the Buchans area (Newfoundland), and showed that the amphibole compositions could provide useful information to infer the cooling history of the host rock. However, despite the petrological interest of riebeckite and arfvedsonite, there is a paucity of experimental work on the stability of these amphiboles, and no crystal-chemical work on cation ordering as a function of *T*, *P*, and f_{O_2} is available as yet.

* E-mail: dellaven@uniroma3.it
† Presently at: Dipartimento di Scienze della Terra, Università "G. D'Annunzio," I-66013 Chieti Scalo, Italy

0003-004X/05/0809–1375$05.00/DOI: 10.2138/am.2005.1682

Magnesioriebeckite was first synthesized by Ernst (1960), who determined its stability as a function of P, T, and f_{O_2}. Accordingly, at constant f_{O_2} defined by the hematite-magnetite buffer, the amphibole is stable at $T < 920$ °C at any $P > 200$ bar; at higher temperature, magnesioriebeckite is replaced by an assemblage of hematite + magnesioferrite + olivine + orthopyroxene + aegirine + vapor. For more-reducing conditions (defined by the magnetite-wüstite buffer), the thermal stability of the amphibole is lowered slightly. The effect of f_{O_2} on the phase equilibria in this system was investigated by Ernst (1962), the run products being characterized using powder X-ray diffraction (XRD). For a constant $P_{H_2O} = 2$ kbar, Ernst (1963) observed that, under reducing conditions, the sodic amphibole produced had a composition richer in FeO, and actually represented solid-solution between magnesioriebeckite and magnesio-arfvedsonite. Scaillet and McDonald (2001, 2003) described the variation in mineral assemblages and composition obtained as a function of f_{O_2} and T in alkali-rich rhyolites. In their study, the appearance of sodic amphibole in the run assemblage was restricted to low f_{O_2} conditions, whereas for higher f_{O_2}, the amphibole was replaced by sodic clinopyroxene (aegirine). More recently, Iezzi et al. (2003a) synthesized the complete solid-solution between ferri-clinoferroholmquistite [$\square Li_2Fe^{2+}_3Fe^{3+}_2Si_8O_{22}(OH)_2$] and riebeckite, and showed that complete replacement of ^{B}Li with ^{B}Na is possible in these amphiboles at 500 °C, 0.4 GPa and moderately reducing conditions (close to NNO), and that an amphibole very close to end-member riebeckite is stable at those conditions.

In this paper, we present the results of experiments done on the bulk magnesioriebeckite composition at $700 < T < 800$ °C and constant $P = 0.4$ GPa under four different f_{O_2} conditions. We then characterize the experimental products, in particular the amphibole site occupancies, by a combination of microchemical and spectroscopic methods.

Experimental and analytical methods

The starting materials were prepared as silicate gels (Hamilton and Henderson 1968). Hydrothermal syntheses (see Table 1 for experimental details and sample labels) were done in internally heated pressure vessels at ISTO-CNRS, Orléans (France). The vessels were fitted with a Shaw membrane to control hydrogen fugacity during the experiment (Scaillet et al. 1992); the f_{O_2} conditions were imposed using different Ar-H_2 gas mixtures (Scaillet et al. 1995, Gaillard et al. 2001, Iezzi et al. 2003b). The temperature was monitored by three sheathed type-K thermocouples placed around the hot spot, with a T gradient within ±5 °C. The pressure conditions were recorded continuously by a transducer calibrated against an Heise-Bourdon tube gauge; the estimated error is ±2 MPa (Scaillet and Evans 1999).

Run products were studied by optical microscopy and SEM-EDS. Powder XRD patterns were obtained using a Scintag X1 diffractometer operated in the vertical θ–θ configuration and equipped with Ni-filtered Cu$K\alpha$ radiation and a Si(Li) solid-state detector. Cell dimensions of the synthetic amphiboles were refined by whole-powder-pattern refinement (Rietveld method) using the GSAS program (Larson and Von Dreele 1997).

Table 1. Conditions and sample labels for experiments on the nominal magnesioriebeckite $\square Na_2(Mg_3Fe^{3+}_2)Si_8O_{22}(OH)_2$ composition

Sample	T (°C)	P (GPa)	f_{O_2} (log NNO)	Duration (days)	Run assemblage (%)*
375	750	0.4	NNO	12	amp 87, qz 13, cpx 0
401	800	0.4	NNO+1	7	amp 94, qz 6, cpx 0
212	750	0.4	NNO+1.5	12	amp 84, qz 13, cpx 1
313	700	0.4	NNO+2.3	12	amp 89, qz 10, cpx 1

Notes: Amp = amphibole, qz = quartz, cpx = clinopyroxene.
* From Rietveld analysis of the powder pattern.

Wavelength-dispersive electron-microprobe analyses were done at the Bayerisches GeoInstitut with a CAMECA SX-50 operating at the following conditions: 15 kV excitation voltage, 10 nA beam current, 20 s counting time on peak, and 10 s counting time on background. The electron-beam spot size was less than 2 µm. The following natural minerals were used as standards: albite (Na and Si, TAP), enstatite (Mg, TAP) and metallic iron (Fe, LiF); data reduction was done with the PAP method (Pouchou and Pichoir 1985).

Powder FTIR spectra were collected in the OH-stretching region (4000–3000 cm^{-1}) at room temperature using a Nicolet 760 spectrophotometer equipped with a DTGS detector and a KBr beamsplitter. Nominal resolution was 2 cm^{-1}; final spectra are the average of 64 scans. Samples were prepared as KBr pellets.

Transmission ^{57}Fe Mössbauer data were acquired at room temperature (298 ± 2 K) using an apparatus in horizontal arrangement (^{57}Fe Co/Rh single-line thin source, constant acceleration mode with symmetric triangular velocity shape, multichannel analyzer with 1024 channels, regular velocity calibration against α-Fe). All spectra were analyzed using the full static hyperfine interaction Hamiltonian analysis with Lorentzian-shaped doublets. Details of the procedures for sample preparation and data handling can be found in Redhammer and Roth (2002).

Experimental products

Quantitative evaluation of the assemblages in the run products was obtained by Rietveld analysis of the powder spectra. In all experiments, a high amphibole yield was obtained, consisting of >85% amphibole plus minor quartz and very minor clinopyroxene (which is, however, found at high f_{O_2}, Table 1). The synthetic amphiboles produced are generally acicular, on average 0.2–0.4 µm across and 2–3 µm in length, with few crystals exceeding these dimensions (Fig. 1). As previously noted for other amphibole systems (Iezzi et al. 2004), the crystal size is strongly

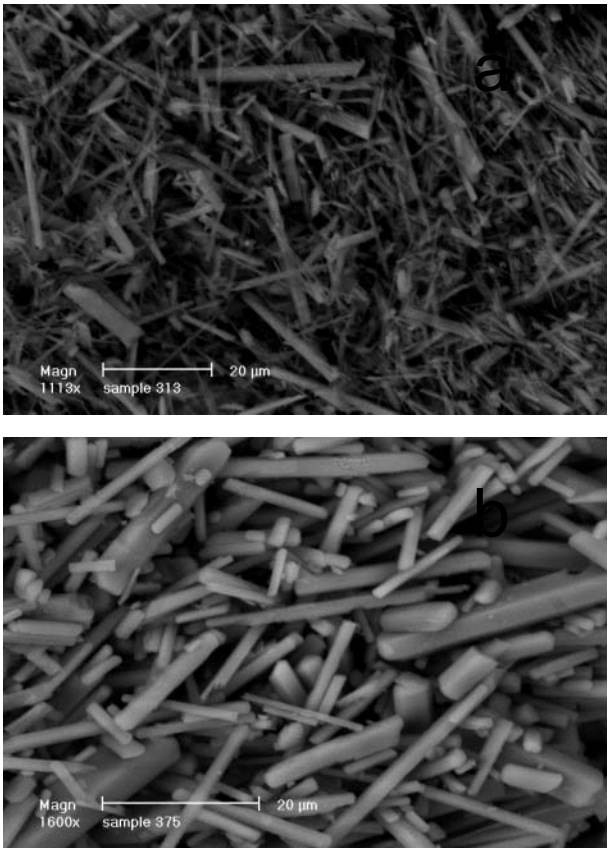

Figure 1. SEM-BSE images of the synthesized amphiboles: (**a**) sample 313, (**b**) sample 375. The scale bar is 20 µm for both samples.

affected by experimental conditions, especially the redox state; the lower f_{O_2} experiments (375 and 401) yielded amphibole crystals with dimensions almost one order of magnitude larger than experiments at higher f_{O_2} (Fig. 1).

CELL PARAMETERS

Powder XRD patterns were indexed in the space group *C*2/*m*, using the fluororiebeckite data (Hawthorne 1978) as a starting model. The resulting refined unit-cell data are summarized in Table 2. The observed differences reflect the variable compositions of the amphiboles synthesized under different redox conditions. However, they are difficult to model in terms of a single crystal-chemical parameter because (as shown later) the product amphiboles show variation at all structural sites as a function of f_{O_2}. The decrease of the *a* edge is clearly related to the significant decrease in the A-site occupancy with increasing f_{O_2} conditions of synthesis (see below), whereas the decrease in the *b* edge for increasing f_{O_2} can be related to the increase in octahedral Fe^{3+}. The slight variation in the β angle is related to the variation in the M4 occupancy. The cell-volume shows a well-defined decrease as a function of f_{O_2}, and is related linearly (Fig. 2) to the A-site occupancy.

There has been much work in the past on the relationship between cell-dimensions and chemical composition of sodic amphiboles. The cell parameters of riebeckites have been studied by Ernst (1962), Borg (1967), and Hoffmann and Katz (1982); the cell parameters of synthetic magnesioriebeckites have been reported by Ernst (1963) and Colville et al. (1966); and the cell-parameters of arfvedsonite have been studied by Frost (1963), Kempe (1969), Afonina et al. (1969), and Koslowski and Hinrichsen (1979). Figure 2 shows the variation of the cell volumes for the (magnesio)riebeckite–(magnesio) arfvedsonite system. Selected data for end-member compositions are summarized in Table 3. Along the magnesioriebeckite–riebeckite series, there is a well-developed change in cell volume as a function of Mg/Fe^{2+} content of the amphibole (Hoffmann and Katz 1982). A similar change is also present in Mg-Fe^{2+} arfvedsonites (Kempe 1969). Connection of the end-member compositions along the arfvedsonite–riebeckite and magnesio arfvedsonite–magnesioriebeckite joins gives cell volume variations for the ideal $^{A}\square$-^{A}Na solid-solution for these amphiboles. The trends are parallel, as expected, and the bulk decrease in cell-volume for both series is ~6 Å^3. The same value is measured for the richterite-tremolite synthetic pairs, both sodic and potassic (data from Robert et al. 1989 and Hawthorne et al. 1997). This observation suggests that the variation in volume in these monoclinic amphiboles is not a simple function of the size of the A-site cation.

The oblique trend of the cell-volume for the amphiboles synthesized here can be rationalized by considering two chemical (and structural) variables acting simultaneously, i.e., $^{A}\square$-^{A}Na solid-solution at the A-site and Mg-Fe^{2+} solid-solution at the C-group sites. An interesting point in Figure 2 is that the trend in cell-volume extrapolates exactly to the magnesioriebeckite composition, suggesting that end-member magnesioriebeckite is stable only at very high f_{O_2} conditions. Note that the cell-volumes given by Ernst (1962, 1963) for nominally end-member riebeckite and magnesioriebeckite (Table 3), both synthesized under very oxidized conditions (hematite-magnetite buffer), show significant deviation from the expected stoichiometry when plotted on our diagram of Figure 2. This finding suggests that the amphiboles synthesized by Ernst (1962, 1963) are in fact riebeckite-arfvedsonite solid-solutions, and that magnesioriebeckite probably has never been obtained experimentally.

TABLE 2. Unit-cell parameters for amphiboles synthesized under different conditions

Sample	*a* (Å)	*b* (Å)	*c* (Å)	β (°)	*V* (Å^3)
375	9.8144(2)	18.0236(6)	5.3062(2)	103.236(3)	913.70(5)
401	9.7747(2)	18.0369(7)	5.3059(2)	103.105(3)	911.10(6)
212	9.7760(2)	17.9754(7)	5.3072(2)	103.448(3)	907.06(5)
313	9.7667(2)	17.9722(7)	5.3100(3)	103.501(3)	906.42(5)

Note: Samples are arranged in increasing values of f_{O_2}.

TABLE 3. Selected unit-cell parameters for amphiboles in the (magnesio)riebeckite–(magnesio)–arfvedsonite system

Sample	*a* (Å)	*b* (Å)	*c* (Å)	β (°)	*V* (Å^3)
(1)	9.73	17.95	5.30	103.3	901
(2)	9.73	18.06	5.33	103.3	913
(3)	9.773(1)	18.078(2)	5.3319(7)	103.40(1)	916.51
(4)	9.82	17.92	5.27	104.0	900
(5)	9.90	18.10	5.33	104.3	925

Notes: (1) magnesioriebeckite, synthetic (Ernst 1963); (2) riebeckite, synthetic (Ernst 1962); (3) riebeckite, synthetic, sample 237 (Iezzi et al. 2003a); (4) magnesio-arfvedsonite, extrapolated from the curves of Kempe (1969); (5) arfvedsonite, estrapolated from the curves of Kempe (1969).

ELECTRON-MICROPROBE ANALYSIS

Due to grain-size limitations, only two samples (375 and 401) could be analyzed by EMPA. Average compositions (>30 points for each sample) of these two amphiboles are compared in Table 4 with stoichiometric magnesioriebeckite. The crystal-chemical formulae were calculated on the basis of 23 O atoms, and Fe_2O_3/FeO was derived by Mössbauer spectroscopy (see below). Values of wt% H_2O needed to give 2 OH in the formula unit are also given in brackets. Exchange reactions involving hydrogen,

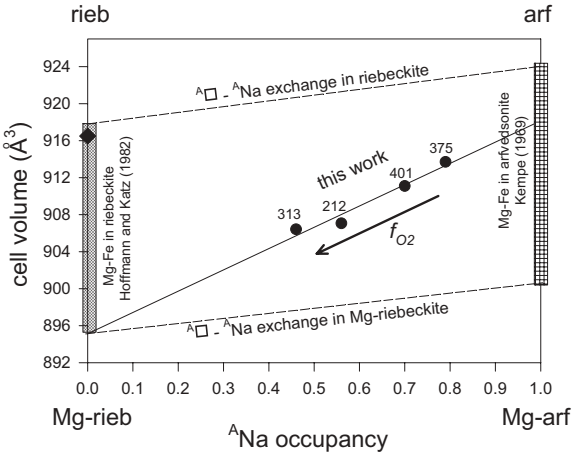

FIGURE 2. Relation between the cell-volume and the A-site occupancy (from Table 8, see text) for the synthesized amphiboles. The line through the data points is a regression line. The arrow shows increasing f_{O_2} of synthesis. The stippled areas along the ordinate represent the range of cell-volume variation for (Mg,Fe^{2+})-riebeckite (Hoffmann and Katz 1982) and (Mg,Fe^{2+})-arfvedsonite (Kempe 1969) systems, respectively. Filled diamond: synthetic end-member riebeckite, from Iezzi et al. (2003a). The broken lines represent the cell-volume variations for the ideal $^{A}\square$-^{A}Na solid-solution.

such as $Fe^{2+} + OH^- = Fe^{3+} + O^{2-}$ (e.g., Popp et al. 1995a, 1995b), in principle could occur in the studied amphiboles. These substitutions have strong effects on the IR OH-stretching spectra, due to local OH-O^{2-} anionic environments in the structure (Della Ventura, unpublished data). Such perturbations are not visible in the spectra collected for the synthesized amphiboles (see below); therefore, we can confidently assume an anionic composition of 2 OH pfu in all samples described here.

The data of Table 4 show that the amphiboles depart strongly from the nominal composition; there is significant $^{C}Fe^{2+}$ and $^{B}(Mg,Fe^{2+})$, and there is extensive ^{A}Na, i.e., an extensive departure of the amphibole composition toward arfvedsonite. According to the Leake et al. (1997) classification scheme, both amphiboles are classified as magnesio-arfvedsonite as $Mg/(Mg + Fe^{2+}) > 0.5$ and $^{A}Na > 0.5$ apfu. However, sample 401 (Table 4) has $^{B}Na < 1.5$ and $^{B}M^{2+} > 0.50$ apfu; therefore, following the new nomenclature recently approved for amphiboles (Leake et al. 2004), it is neither a sodic (defined by having $^{B}Na > 1.5$ apfu), nor a sodic-calcic amphibole, as it has no Ca in the formula, but is a member of the new group 5 defined by the $0.5 < {}^{B}(Mg, Fe^{2+}, Mn^{2+}, Li) < 1.50$ and $0.50 \le {}^{B}(Ca, Na) \le 1.50$ limits (Leake et al. 2004). The compositions of samples 375 and 401 can be expressed by the combination of two exchange vectors:

$$^{C}(Mg,Fe^{2+})\ ^{B}(Mg,Fe^{2+})\ ^{C}Fe^{3+}_{-1}\ ^{B}Na_{-1} \quad (1)$$

and

$$^{A}Na\ ^{C}(Mg,Fe^{2+})\ ^{A}\square_{-1}\ ^{C}Fe^{3+}_{-1} \quad (2).$$

Exchange vector 1 has been recently described for the closely related ferri-clinoholmquistite system (Iezzi et al. 2004), while exchange vector 2 accounts for the filling of the A-site along the series. This point will be discussed below in more detail.

TABLE 4. EMP analyses (averages of > 30 point analyses) and crystal-chemical formulae based on 23 oxygen atoms pfu for the synthesized amphiboles

	Ideal	375	401
SiO_2 (wt%)	57.14	54.63(0.4)	55.23(0.6)
Fe_2O_3	18.98	7.83(0.4)	8.05(0.6)
FeO	00.00	13.26(0.4)	11.96(0.6)
MgO	14.37	13.38(0.4)	15.12(0.6)
Na_2O	7.37	8.8(0.4)	7.71(0.2)
H_2O	(2.14)	(2.06)	(2.08)
Total	100.00	99.96	100.15
Si (apfu)	8.00	7.97	7.96
Fe^{3+}	2.00	0.86	0.87
Fe^{2+}	0.00	1.62	1.42
Mg	3.00	2.91	3.25
Σc	5.00	5.39	5.54
c-5	0.00	0.39	0.54
^{B}Na	2.00	1.61	1.46
^{A}Na	0.00	0.88	0.70
OH	(2.00)	(2.00)	(2.00)
OS	1.00	0.35	0.38

Notes: Fe^{3+}/Fe^{2+} from Mössbauer; e.s.d. in brackets. H_2O in brackets calculated to give 2 OH apfu. OS = oxidation state = $Fe^{3+}/Fe_{(T)}$.

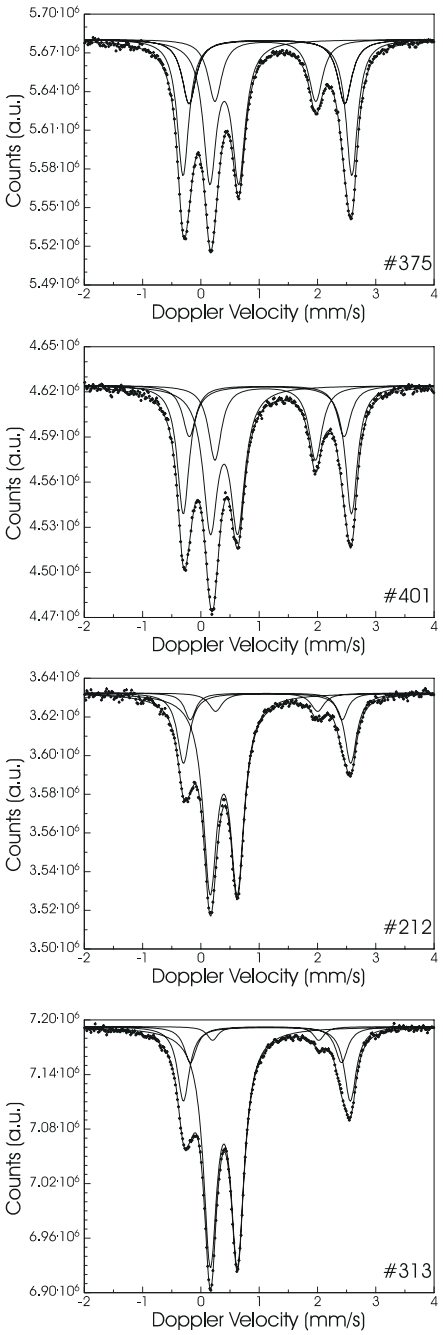

FIGURE 3. Fitted Mössbauer spectra for the synthesized amphiboles.

MÖSSBAUER SPECTROSCOPY

Description of the spectra

The fitted Mössbauer spectra are displayed in Figure 3. The spectra consist of five well-resolved resonance absorption lines. The lines centered at ~ +0.2 and ~ +0.55 mm/s give rise to quadrupole doublets (see Table 5) having isomer shifts of ~0.39 mm/s and quadrupole splittings of ~0.47 mm/s, values

TABLE 5. ^{57}Fe hyperfine parameters at 298(2) K for thickness-corrected Mössbauer spectra derived from Lorentzian - shaped doublet analysis using the complete static hyperfine interaction Hamiltonian

Sample	c^2	IS (mm/s)	QS (mm/s)	G (mm/s)	A (%)	Assignment
375	0.528	0.402	0.497	0.135	34.7(5)	Fe^{3+} M2
		1.142	2.895	0.122	31.2(7)	Fe^{2+} M1
		1.132	2.671	0.144	17.5(8)	Fe^{2+} M3
		1.106	1.731	0.143	16.6(8)	Fe^{2+} M4
401	0.642	0.398	0.468	0.149	38.1(5)	Fe^{3+} M2
		1.141	2.886	0.124	30.1(7)	Fe^{2+} M1
		1.129	2.654	0.138	13.1(8)	Fe^{2+} M3
		1.104	1.725	0.135	18.7(9)	Fe^{2+} M4
212	0.692	0.392	0.468	0.142	64.9(6)	Fe^{3+} M2
		1.136	2.868	0.125	21.5(8)	Fe^{2+} M1
		1.120	2.597	0.115	7.5(8)	Fe^{2+} M3
		1.127	1.751	0.136	6.1(9)	Fe^{2+} M4
313	0.629	0.394	0.467	0.140	67.0(5)	Fe^{3+} M2
		1.132	2.863	0.124	19.7(7)	Fe^{2+} M1
		1.116	2.592	0.129	10.0(7)	Fe^{2+} M3
		1.112	1.821	0.112	3.3(9)	Fe^{2+} M4

typical for Fe^{3+} in the high-spin state. The spectra show that in our synthetic amphiboles, Fe^{3+} occupies exclusively one single site as there are no signs for other Fe^{3+} doublets. The resonance absorption line at ~ +2.0 mm/s and an absorption line at ~ +0.2 mm/s, which is superimposed on the dominating Fe^{3+} line, give rise to a quadrupole doublet with an isomer shift of 1.10(2) mm/s and a quadrupole splitting of 1.75(1) mm/s. This doublet is assigned to Fe^{2+}. The two outermost lines are also characterized by ^{57}Fe hyperfine parameters typical of Fe^{2+} in the high-spin state. However, two doublets/components have to be used to model these slightly asymmetric outermost resonance absorption lines adequately (Fig. 3). These two doublets show quadrupole splitting values of 2.837(5) and 2.54(2) mm/s. On the basis of previous studies (e.g., Hawthorne 1983; Redhammer and Roth 2002; Iezzi et al. 2003a, 2003b, 2004), Fe^{3+} is assigned to the M2 site, whereas the two Fe^{2+} doublets having quadrupole splitting values of 2.837 mm/s and 2.54 mm/s are assigned to the M1 and M3 sites, respectively. The well-resolved fourth doublet, found in all magnesioriebeckite spectra of this study, exhibits a quadrupole splitting of ~1.8 mm/s, which is too low to be assigned to the M2 site. Thus, this resonance absorption contribution is assigned to Fe^{2+} at the M4 site. A doublet with very similar hyperfine parameters recently has been observed by Iezzi et al. (2004) in synthetic ferri-clinoferroholmquistite, and was also described by Redhammer and Roth (2002) for synthetic Fe-rich richterite.

Site-occupancies from Mössbauer data

Analysis of the Mössbauer spectra (Table 5) shows that in our synthetic amphiboles, Fe^{3+} is completely ordered at M2, and Fe^{2+} is disordered at the M1, M3, and M4 sites. No $^{M2}Fe^{2+}$ could be detected. The relative amounts of Fe^{2+} and Fe^{3+} are strongly variable as a function of f_{O_2}: for increasing oxidation conditions, there is a strong increase in $^{M2}Fe^{3+}$ and a decrease in Fe^{2+}, as expected; however, the most significant decrease is shown by Fe^{2+} at M4. In addition, Mössbauer spectroscopy shows that $^{C}Fe^{2+}$ is almost equally disordered between M1 and M3 at any f_{O_2}. The same feature was also observed by Iezzi et al. (2004) for synthetic ferri-holmquistite.

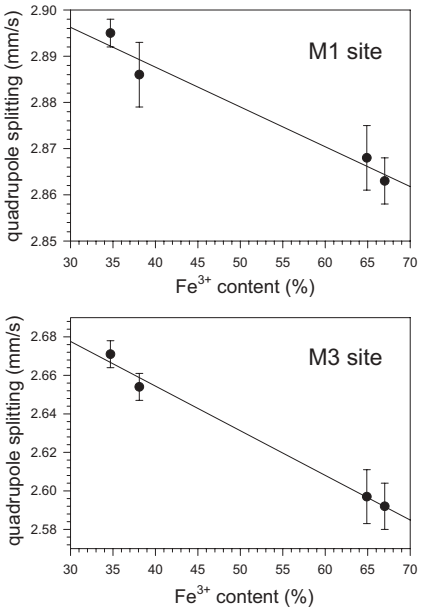

FIGURE 4. $^{M1,M3}Fe^{2+}$ Quadrupole splitting vs. Fe^{3+} content for the amphiboles synthesized in the present work.

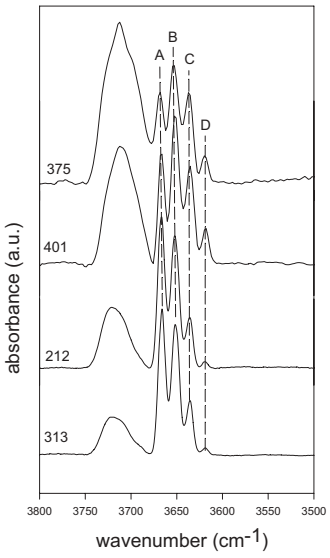

FIGURE 5. OH-stretching IR spectra for the synthesized amphiboles. Samples are arranged in order of increasing oxygen fugacity from top to bottom.

Variation in ^{57}Fe hyperfine parameters

Besides the variation in Fe concentrations over the available sites, the data of Table 5 show distinct changes in ^{57}Fe hyperfine parameters, notably the quadrupole splitting, as a function of Fe^{3+} content in the amphibole. This feature is evident for Fe^{2+} at both M1 and M3, where the quadrupole splitting is linearly correlated with $^{M2}Fe^{3+}$ (Fig. 4), and is consistent with the findings of Hawthorne (1983) and Redhammer and Roth (2002) who noticed

a correlation between the size of the Fe^{2+} quadrupole splitting at M1 and M3 and the mean ionic radius of the M2 site. The quadrupole splitting of Fe^{2+} is known to be inversely related to the distortion of the octahedron occupied by the probe nucleus, and the plots of Figure 4 suggest an increase in the geometric/electronic distortion of the M(1,3) octahedra with increasing $^{M2}Fe^{3+}$ in the amphibole.

INFRARED SPECTROSCOPY

Description of the spectra

The OH-stretching FTIR spectra collected for these synthetic samples are given in Figure 5. All spectra show a well-defined quadruplet of rather sharp (FWHM = 9–10 cm^{-1}) bands, denoted A to D in Figure 5, centered at 3669, 3653, 3637, and 3619 cm^{-1}, respectively, and a very broad absorption at >3700 cm^{-1}. In the amphiboles examined here, the four sharp bands (A-D) can be assigned to the various combinations of Mg-Fe^{2+} at M(1,3) (e.g., Strens 1966; Burns and Strens 1966; Della Ventura 1992; Della Ventura et al. 1996; Reece et al. 2002); in particular, the A band is assigned to the MgMgMg-OH-$^{A}\square$ configuration, the B band to the MgMgFe^{2+}-OH-$^{A}\square$ configuration, the C band to the Mg$Fe^{2+}Fe^{2+}$-OH-$^{A}\square$ configuration, and the D band to the $Fe^{2+}Fe^{2+}Fe^{2+}$-OH-$^{A}\square$ configuration. Visual inspection of the spectra in Figure 5 shows that there is an evolution in the relative intensity of these components throughout the series, suggesting a variation in the relative Mg/Fe^{2+} content at M(1,3) as a function of f_{O_2}.

The broad absorption centered at >3700 cm^{-1} can be assigned to occupied A-site configurations (Della Ventura 1992; Della Ventura et al. 2003). It consists of several overlapping components, as suggested by the shoulders apparent on both sides of the peak centroid; its bulk intensity is inversely related to the f_{O_2} of synthesis: it is a maximum for sample 375 obtained under reducing conditions, whereas it is less intense for sample 313, obtained under very oxidizing conditions.

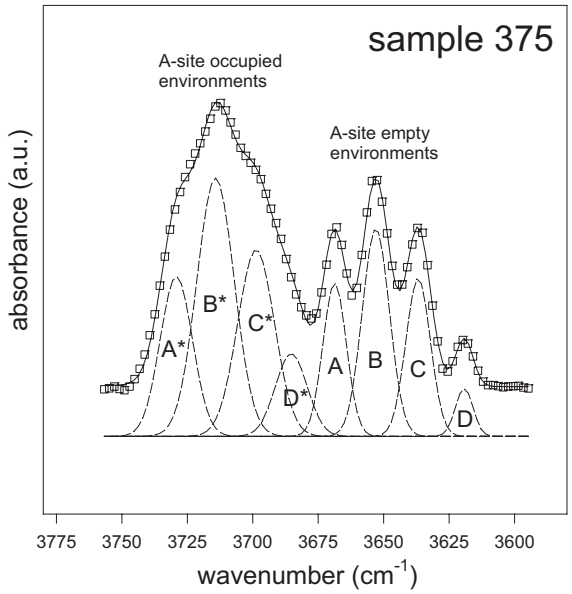

FIGURE 6. The fitted spectrum of sample 375. The component labels are indicated.

Site-occupancies from FTIR data

A quantitative evaluation of the site occupancy for two cations (in this case Mg and Fe^{2+}) at the OH-coordinated M1 and M3 sites of the synthesized amphiboles, is provided by the intensities (areas) of the bands in the IR OH-stretching region (Hawthorne et al. 1996; Della Ventura et al. 1996; Iezzi et al. 2004). The relative intensities of the bands in the spectrum of Figure 5 have been measured by fitting Gaussian components (Della Ventura et al. 1996) to the spectrum. One example of such a fitting is shown in Figure 6. The well-resolved quartet of bands <3680 cm^{-1} (Fig. 5) can be modeled easily using four symmetrical Gaussian components, and there is a rapid convergence during unconstrained refinement. However, the broad absorption at >3680 cm^{-1}, which is evidently due to several overlapping bands, does not contain sufficient information to allow unconstrained fitting of component bands and we were forced to constrain some parameters during the fitting process. Peak-shape parameters initially were derived for sample 375, where the broad band (and thus the hyperfine components) is more prominent, and then fixed during the preliminary refinement cycles for all other spectra. In all samples, bands A* and B* (Fig. 6) could be refined unconstrained, whereas for the less-intense C* and D* bands, the position and/or width were fixed in such a way to reproduce, for

TABLE 6. Positions (cm^{-1}), widths (cm^{-1}) and relative intensities for the component bands in the OH-spectra of the synthesized amphiboles

Band	Parameter	375	401	212	313
A	Position (cm^{-1})	3669	3667	3667	3666
	Width	10.5	8.0	8.9	9.0
	Intensity (%)	0.09	0.11	0.26	0.29
B	Position (cm^{-1})	3653	3652	3652	3651
	Width	12.2	10.5	10.8	10.0
	Intensity (%)	0.15	0.20	0.28	0.30
C	Position (cm^{-1})	3637	3636	3636	3636
	Width	11.1	11.2	8.7	9.0
	Intensity (%)	0.10	0.14	0.08	0.11
D	Position (cm^{-1})	3619	3618	3619	3619
	Width	7.9	8.4	5.9	9.0
	Intensity (%)	0.02	0.04	0.01	0.01
A*	Position (cm^{-1})	3729	3725	3725	3726
	Width	14.5	14.1	18.1	18.1
	Intensity (%)	0.14	0.13	0.18	0.13
B*	Position (cm^{-1})	3714	3712	3712	3712
	Width	16.8	15.1	17.0	17.0
	Intensity (%)	0.25	0.20	0.13	0.10
C*	Position (cm^{-1})	3699	3699	3701	3701
	Width	16.6	14.9	13.4	13.4
	Intensity (%)	0.18	0.13	0.05	0.03
D*	Position (cm^{-1})	3685	3689	3690	3690
	Width	14.3	13.5	11.9	11.9
	Intensity (%)	0.07	0.05	0.01	0.02

TABLE 7. IR-derived site-populations at M(1,3) and at the A-site for the synthesized amphiboles

		375	401	212	313
$^{A}\square$-M(1,3)	Mg	0.67	0.87	1.42	1.60
	Fe^{2+}	0.41	0.60	0.47	0.56
^{A}Na-M(1,3)	Mg	1.10	0.92	0.85	0.62
	Fe^{2+}	0.82	0.61	0.26	0.22
^{Tot}M(1,3)	Mg	1.77	1.79	2.27	2.22
	Fe^{2+}	1.23	1.21	0.73	0.78
A-site	Na	0.80	0.70	0.56	0.46
	$\square$	0.20	0.30	0.44	0.54

the A*-D* bands, a relative frequency separation similar to that observed for the A-D bands. The final refined band positions, widths and intensities are summarized in Table 6.

The relative intensity data of Table 6 were then used to calculate the octahedral site occupancies, using the equations of Burns and Strens (1966):

$$^{M1,3}Mg = 3I_A + 2I_B + I_C \text{ and } ^{M1,3}Fe^{2+} = I_B + 2I_C + 3I_D$$

where I_i are the measured intensities of the resolved bands. Note that $I_A = I_A + I_{A*}$, $I_B = I_B + I_{B*}$, etc. Estimation of vacant vs. occupied A-site environments in the synthesized amphiboles was done following the method of Hawthorne et al. (1997), established for synthetic richterite-tremolite solid-solutions. Accordingly, the mole fraction of A-site-vacant environment (X_{tr}) can be derived from the relative intensity of the bands in the IR spectrum using the equation $X_{tr} = R/[k + R(1 - k)]$ (Hawthorne et al. 1997) where R is the measured relative intensity ratio between the A-site vacant ($I_A + I_B + I_C + I_D$) and the A-site filled ($I_{A*} + I_{B*} + I_{C*} + I_{D*}$) environment and k = 2.2 is the correction factor for the difference in molar absorptivity. The site populations obtained are summarized in Table 7.

THE MAGNESIO-RIEBECKITE–MAGNESIO-ARFVEDSONITE SOLID-SOLUTION AS A FUNCTION OF f_{O_2}

As the sizes of the synthesized crystals are not always suitable for reliable EMP analysis, details on their crystal chemistry are based on spectroscopic measurements. As shown by Iezzi et al. (2004), combined use of Mössbauer and FTIR provides results strongly coherent with direct techniques such as EMPA and single-crystal XRD. For the amphiboles presented here, we have EMPA data for two samples, and the results for these samples can be used as a preliminary test of the accuracy of the spectroscopically derived data for the remaining samples. The final site occupancies obtained by combining the different techniques are compared in Table 8. There is excellent agreement between the data obtained from EMPA (combined with Mössbauer for the Fe^{3+}/Fe^{2+} ratio) and the composition derived combining FTIR and Mössbauer spectroscopies. In particular, there is good agreement in the A-site occupancy data, indicating that the model of Hawthorne et al. (1997) is reasonable and that k = 2.2 is a suitable correction factor in the system examined here. The good agreement between the EMPA and the FTIR-derived Mg/Fe^{2+} composition at M(1,3) allows us to use the IR data as a basis for calculating the complete crystal-chemical formulae for all amphiboles from the relative distribution of Fe^{3+} and Fe^{2+} at the C- and B-sites (Mössbauer), a feature that is of particular importance for those samples where EMPA data cannot be collected.

The data of Table 8 show that the amphiboles synthesized depart strongly from the nominal composition, and that end-member magnesioriebeckite is *not* stable under the *P-T-*f_{O_2}conditions investigated here. In particular, there is a well-defined relation between the f_{O_2} of synthesis and ^{A}Na (Fig. 7); increasingly reducing conditions favor the entry of Na into the A-site and stabilize the arfvedsonite component in solid-solution within magnesioriebeckite. These conclusions are in agreement with the work of Ernst (1962) on the riebeckite-arfvedsonite relations. However, although the riebeckite–arfvedsonite relations primarily are correlated with the amount of Fe^{3+} in the amphibole structure, which controls the amount of ^{A}Na via the $^{A}Na\ ^{C}(Mg,Fe^{2+})\ ^{A}\square_{-1}\ ^{C}Fe^{3+}_{+1}$ exchange vector, the crystal chemistry in this system ultimately is controlled by a more-complex exchange vector that can be expressed as:

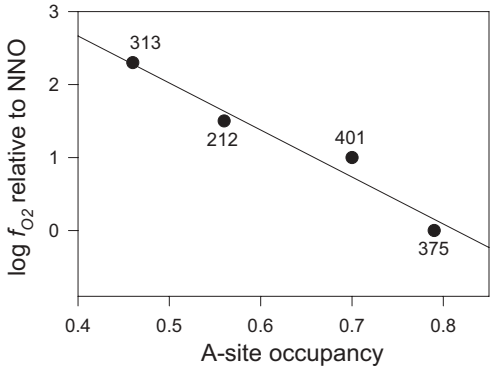

FIGURE 7. Relation between the A-site occupancy derived by FTIR spectroscopy and the log f_{O_2} relative to NNO for the synthesized amphiboles.

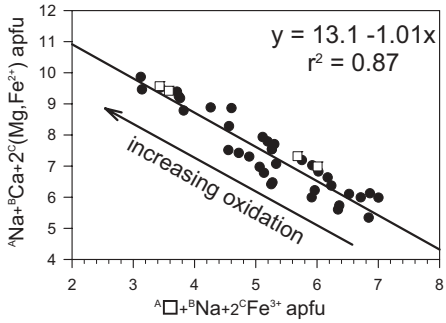

FIGURE 8. Plot of the $^{C}(Mg,Fe^{2+})\ ^{B}(Mg,Fe^{2+})\ ^{C}Fe^{3+}_{+1}\ ^{B}Na_{-1}$ vs. the $^{A}Na\ ^{C}(Mg,Fe^{2+})\ ^{A}\square_{-1}\ ^{C}Fe^{3+}_{+1}$ contents for chemical analyses of alkali amphiboles in the mineralogical literature (filled circle), from Kovalenko (1968) and Deer et al. (1997). Hollow square = synthetic amphiboles from this study. For explanation see text.

TABLE 8. Final site-populations for all synthesized amphiboles combining EMPA, Mössbauer and FTIR data

Sample		375		401		212	313
site		EMPA Möss	IR	EMPA Möss	IR	Möss IR	Möss IR
M1	Mg	1.22	–	1.34	–	1.46	1.49
	Fe^{2+}	0.78	–	0.66	–	0.54	0.51
M3	Mg	0.56	–	0.71	–	0.81	0.73
	Fe^{2+}	0.44	–	0.29	–	0.19	0.27
$\Sigma_{M1,3}$	Mg	1.78	1.77	2.05	1.79	2.27	2.22
	Fe^{2+}	1.22	1.23	0.97	1.21	0.73	0.78
M2	Mg	1.14	–	1.13	–	0.30	0.22
	Fe^{3+}	0.86	–	0.87	–	1.70	1.78
M4	Na	1.6	–	1.5	–	1.84	1.91
	Mg	–	–	0.07	–	–	–
	Fe^{2+}	0.4	–	0.43	–	0.16	0.09
A	Na	0.89	0.80	0.66	0.70	0.56	0.46
OS		0.35		0.38		0.65	0.67

Note: OS (oxidation state) = Fe^{3+}/Fe_{tot}.

$^{A}Na\ ^{B}(M^{2+})\ ^{C}(Mg,Fe^{2+})_2\ ^{A}\square_{-1}\ ^{B}Na_{-1}\ ^{C}Fe^{3+}_{-2}$, where M^{2+} = Ca, Mg, Fe^{2+}.

In natural systems, M^{2+} is almost exclusively Ca, but in Ca-free synthetic systems, M^{2+} can be Mg and/or Fe^2 or Mn^{2+}. Figure 8 displays a plot of the above exchange vector for the amphiboles synthesized here together with the data for many alkali amphibole analyses in the mineralogical literature. Note that the linear regression of the data plotted on Figure 8 has a slope of –1, lending support to the above substitutional vector.

PETROLOGICAL IMPLICATIONS

Strong and Taylor (1984) suggested that there are two distinct compositional trends in alkali amphiboles from silica-saturated peralkaline igneous rocks: (1) a *magmatic-subsolidus trend* that involves amphiboles with fully A-sites (barroisite/katophorite to richterite to arfvedsonite) and is proposed to occur under reducing conditions; and (2) an *oxidation trend* that involves changes toward alkali amphiboles with vacant A-sites and Fe^{3+} at M2 (riebeckite), under the influence of oxidizing hydrothermal fluids. These empirical trends are in accordance with the results of Figure 7 where it is shown that the A-site occupancy is inversely related to the oxygen fugacity. However, Czamanske and Wones (1973), Czamanske et al. (1977, 1981), and Czamanske and Dillet (1988) among others, have clearly shown that, during magmatic crystallization, trends in amphibole compositions may reflect either progressively oxidizing or reducing conditions. Also, the experimental results of Scaillet and MacDonald (2001, 2003) demonstrate that extreme oxidation of silicic alkali magmas leads to amphibole breakdown in favor of clinopyroxene, implying that an increase in f_{O_2} does not necessarily promote amphibole crystallization. A further problem in this context is the common presence of ^{C}Li in alkali amphiboles whose omission in the analysis leads to significant errors in the formula calculation and in the estimation of the Fe^{3+}/Fe^{2+} ratio (and thus of the oxidation state) (Hawthorne et al. 1993).

Our experimental results show a well-defined inverse relation between A-site occupancy and oxygen fugacity (in the absence of Li), are in accord with documented natural occurrences. This finding suggests that amphibole composition may be used to monitor the f_{O_2} conditions during crystallization, as noticed by King et al. (2000) for basanitic melts. However, we stress that oxygen fugacity is not the unique parameter controlling the amphibole composition. For instance, Scaillet and Macdonald (2003) have shown that water fugacity also plays a key role: in alkali-rich, silicic magmas, at fixed P-T-f_{O_2} conditions, an increase in f_{H_2O} strongly promotes the increase in the Ca content of the alkali-amphibole.

ACKNOWLEDGMENTS

The syntheses were done during the Ph.D. work of G.I. at I.S.T.O.-CNRS, Orléans (France), financed by an EGIDE-Italian Ministry of Foreign Affairs. The post-doc stay of GI at Bayerisches GeoInstitut was financed by a Sofja Kovalevskaja Program. Thanks are due to Detlef Krauβe for helping during the microprobe analyses. G.J.R. thanks G. Amthauer for providing the Mössbauer equipment for this study and the Austrian "Fonds zur Förderung der Wissenschaftlichen Forschung" for financial support under grant R33-N10 (Schrödinger-Rückkehr-Programm). A. Mottana gave helpful suggestions during the manuscript preparation. Positive criticism by W. Maresch, D. Jenkins, and B. Evans is also acknowledged.

REFERENCES CITED

Afonina, G.G., Kovalenko, V.I., and Pisarskaya, V.A. (1969) Composition and lattice parameters of riebeckite–arfvedsonite amphiboles. Doklady Academii Nauk SSSR, Earth Sciences Section, 187, 130–134.

Borg, I.Y. (1967) Optical properties and cell parameters in the glaucophane–riebeckite series. Contribution to Mineralogy and Petrology, 15, 67–92.

Borley, G.D. (1963) Amphiboles from the younger granites of Nigeria. Part I. Chemical classification. Mineralogical Magazine, 33, 358–576.

Burns, R.G. and Strens, R.G.J. (1966) Infrared study of the hydroxile bands in clinoamphiboles. Science, 153, 890–892.

Colville, P.A., Ernst, W.G., and Gilbert, M.C. (1966) Relationships between the cell parameters and the chemical composition of monoclinic amphiboles. American Mineralogist, 51, 1727–1754.

Czamanske, G.K. and Dillet, B. (1988) Alkali amphibole, tetrasilicic mica and sodic pyroxene in peralkaline siliceous rocks, Questa Caldera, New Mexico. American Journal of Science, 288A, 358–392.

Czamanske, G.K. and Wones, D.R. (1973) Oxidation during magmatic differentiation, Finnmarka complex, Oslo area, Norway. II. The mafic silicates. Journal of Petrology, 14, 349–380.

Czamanske, G.K., Wones, D.R., and Eichelberger, J.C. (1977) Mineralogy and petrology of the intrusive complex of the Pliny Range, New Hampshire. American Journal of Science, 277, 1073–1123.

Czamanske, G.K., Ishahara, S., and Atkin, S.A. (1981) Chemistry of rock-forming minerals of the Cretaceous-Paleocene batholith in Southwestern Japan and implications for magma genesis. Journal of Geophysical Research, 86, 10431–10469.

Deer, W.A., Howie, R.A., and Zussman, J. (1997) Rock forming minerals, Double-chain Silicates. Longman Scientific and Technical, p. 692.

Della Ventura, G. (1992) Recent developments in the synthesis and characterization of amphiboles. Synthesis and crystal chemistry of richterite. Trends in Mineralogy, 1, 153–192.

Della Ventura, G., Robert, J.-L., and Hawthorne, F.C. (1996) Infrared spectroscopy of synthetic (Ni,Mg,Co)-potassium-richterite. In Dyar, M.D., McCammon, C., and Schaefer, E.W., Ed., Mineral Spectroscopy: a Tribute to Roger G. Burns. The Geochemical Society Special Publication No. 5, 55–63.

Della Ventura, G., Hawthorne, F.C., Robert, J.-L., and Iezzi, G. (2003) Synthesis and infrared spectroscopy of amphiboles along the tremolite–pargasite join. European Journal of Mineralogy, 15, 341–347.

Ernst, W.G. (1960) The stability relations of magnesioriebeckite. Geochimica and Cosmochimica Acta, 19, 10–40.

——— (1962) Synthesis, stability relations and occurrence of riebeckite and riebeckite-arfvedsonite solid solutions. Journal of Geology, 70, 689–736.

——— (1963) Polymorphism in alkali amphiboles. American Mineralogist, 48, 241–260.

Frost, M.T. (1963) Amphiboles from the Younger Granites of Nigeria. Part II. X-ray data. Mineralogical Magazine, 33, 377–384.

Gaillard, F., Scaillet, B., Pichavant, M., and Beny, J.M. (2001) The effect of water and f_{O2} on the ferric-ferrous ratio of silicic melts. Chemical Geology, 174, 255–273.

Hamilton, D.L. and Henderson, C.M.B. (1968) The preparation of silicate compositions by a gelling method. Mineralogical Magazine, 36, 832–838.

Hawthorne, F.C. (1978) The crystal chemistry of the amphiboles. VIII. The crystal structure and site chemistry of fluor-riebeckite. Canadian Mineralogist, 16, 187–194.

——— (1983) The crystal chemistry of the amphiboles. Canadian Mineralogist, 21, 173–480.

Hawthorne, F.C., Ungaretti, L., Oberti, R., Bottazzi, P., and Czamanske, G.K. (1993) Li: An important component in igneous alkali amphiboles. American Mineralogist, 78, 733–745.

Hawthorne, F.C., Della Ventura, G., and Robert, J.-L. (1996) Short-range order and long-range order in amphiboles: a model for the interpretation of infrared spectra in the principal OH-stretching region. Geochimica and Cosmochimica Acta, Spec. Vol. 5, 49–54.

Hawthorne, F.C., Della Ventura, G., Robert, J.-L., Welch, M.D., Raudsepp, M., and Jenkins, D.M. (1997) A Rietveld and infrared study of synthetic amphiboles along the potassium-richterite-tremolite join. American Mineralogist, 82, 708–716.

Henley, R.W. (1978) Arfvedsonite in basalt dykes, Buchans, Newfoundland. American Mineralogist, 63, 413–414.

Hoffmann, C. and Katz, K. (1982) Trend surface analysis of some physical properties of alkali (sodic) amphiboles. Lithos, 15, 17–25.

Iezzi, G., Della Ventura, G., Càmara, F., Pedrazzi, G., and Robert, J.L. (2003a) ^{B}Na-^{B}Li solid-solution in A-site-vacant amphiboles: synthesis and cation ordering along the ferri-clinoferroholmquistite-riebeckite join. American Mineralogist, 88, 955–961

Iezzi, G., Della Ventura, G., Pedrazzi, G., Robert, J.L., and Oberti, R. (2003b) Synthesis and characterisation of ferri-clinoferroholmquistite, $Li_2(Fe^{2+}_3$

Fe^{3+}_2)$Si_8O_{22}(OH)_2$, European Journal of Mineralogy, 15, 321–328.
Iezzi, G., Cámara, F., Della Ventura, G., Oberti, R., Pedrazzi, G., and Robert, J.L. (2004) Synthesis, crystal structure and crystal-chemistry of ferri-clinoholmquistite, $\square Li_2Mg_2Fe_3Si_8O_{22}(OH)_2$. Physics and Chemistry of Minerals, 31, 375–385.
Kempe, D.R.C. (1969) The cell parameters of the arfvedsonite–eckermannite series, with observations on the MgO and total iron content of amphiboles. Mineralogical Magazine, 37, 317–332.
King, P.L., Hervig, R.L., Holloway, J.R., Delaney, J.S., and Dyar, M.D. (2000) Partitioning of Fe^{3+}/Fe_{tot} between amphibole and basanitic melt as a function of oxygen fugacity. Earth and Planetary Science Letters, 178, 97–112.
Koslowski, T. and Hinrichsen, T. (1979) Synthesis, properties and upper thermal stability of a glaucophane–riebeckite mixed crystal. Neues Jahrbuch für Mineralogie, Monashefte, (1979), 357–362.
Kovalenko, V.I. (1968) On the chemical composition, properties, and mineral paragenesis of riebeckite and arfvedsonite. Papers and Proceedings, IMA 5th general meeting, Cambridge. The Mineralogical Society, London, 261–284.
Larson, A.C. and Von Dreele, R.B. (1997) GSAS: General Structure Analysis System. Document LAUR 86-748, Los Alamos National Laboratory.
Leake, B.E. et al. (1997) Nomenclature of amphiboles: Report of the Subcommittee on amphiboles of the International Mineralogical Association, Commission on new minerals and mineral names. American Mineralogist, 82, 1019–1037.
——— (2004) Nomenclature of amphiboles: additions and revisions to the International Mineralogical Association's amphibole nomenclature. European Journal of Mineralogy, 16, 190–195.
Lyons, P.C. (1976) The chemistry of riebeckites of Massachusetts and Rhode Island. Mineralogical Magazine, 40, 473–479.
Popp, R.K., Virgo, D., Yoder, H.S.Jr., Hoering, T.S., and Phillips, M.W. (1995a) An experimental study of phase equilibria and Fe oxy-component in kaersutitic amphiboles: implications for the f_{O_2} and a_{H_2O} in the upper mantle. American Mineralogist, 80, 534–548.
Popp, R.K., Virgo, D., and Phillips, M.W. (1995b) H deficiency in kaersutitic amphiboles: experimental verification. American Mineralogist, 80, 1347–1350.
Pouchou, J.L. and Pichoir, F. (1985) 'PAP' $\phi(\rho Z)$ procedure for improved quantitative micro-analysis. Microbeam Analysis, 104–160.
Redhammer, G.J. and Roth, G. (2002) Crystal structure and Mössbauer spectroscopy of the synthetic amphibole potassic ferri-ferrorichterite at 298 K and low temperatures (80–110 K). European Journal of Mineralogy, 105–114.
Reece, J.J., Redfern, S.A.T., Welch, M.D., Henderson, C.M.B., and McCammon, C.A. (2002) Temperature-dependent Fe^{2+}-Mn^{2+} order-disorder behaviour in amphiboles. Physics and Chemistry of Minerals, 29, 562–570.
Robert, J.L., Della Ventura, G., and Thauvin, J.L. (1989) The infrared OH-stretching region of synthetic richterites in the system Na_2O-K_2O-CaO-MgO-SiO_2-H_2O-HF. European Journal of Mineralogy, 203–211.
Scaillet, B. and Evans, B.W. (1999) The June 15, 1991 eruption of Mount Pinatubo: I. Phase equilibria and pre-eruption P-T-f_{O_2}-f_{H_2O} conditions of the dacite magma. Journal of Petrology, 40, 381–411.
Scaillet, B. and McDonald, R. (2001) Phase relations of peralkaline silicic magmas and petrogenetic implications. Journal of Petrology, 42, 825–845.
——— (2003) Experimental constraints on the relationships between peralkaline rhyolites of the Kenya Rift Valley. Journal of Petrology, 43, 1867–1894.
Scaillet, B., Pichavant, M., Roux, J., Humbert, G., and Lefevre, A. (1992) Improvements of the Shaw membrane techniques for measureaments and control of f_{H_2} at high temperatures and pressure. American Mineralogist, 77, 647–655.
Scaillet, B., Pichavant, M., and Roux, J. (1995) Experimental crystallisation of leucogranite magmas. Journal of Petrology, 36, 663–705.
Strens, R.G.J. (1966) Infrared study of cation ordering and clustering in some (Fe, Mg) amphibole solid solutions. Chemical Communications, 15, 519–520.
Strong, D.F. and Taylor, R.P. (1984) Magmatic-subsolidus and oxidation trends in composition of amphiboles from silica-saturated peralkaline igneous rocks. Tschermaks Mineralogisch-Petrologische. Mitteilungen, 32, 211–222.

MANUSCRIPT RECEIVED APRIL 24, 2004
MANUSCRIPT ACCEPTED FEBRUARY 7, 2005
MANUSCRIPT HANDLED BY ALISON PAWLEY